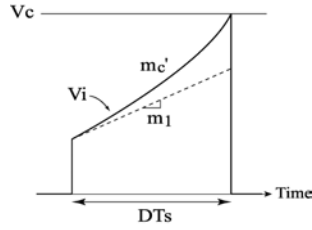


(a) Conceptual V_i and V_c in Fig. 1.



(b) Desired waveforms for V_i and V_c .

Fig. 2. Waveforms at input terminals of the PWM comparator.

control signal for the output voltage, and the I/V converted voltage of a linear compensation slope current is added to V_i instead of V_c , although the linear and negative slope was included in V_c in Figure 2(a).

Consider a step current change in an inductor. The change is transferred to the control voltage V_i , as seen in Figure 2(a). For a sudden inductor current change to be settled, ΔV_2 must be smaller than ΔV_1 . This equals

$$\frac{\Delta V_2}{\Delta V_1} = -\frac{m_2 - m_c}{m_1 + m_c}, \text{ and } |\Delta V_2| < |\Delta V_1| \quad (1)$$

and the condition for m_c becomes

$$m_c > \frac{(2D - 1) V_{in}}{2L} K_{cfb} \quad (2)$$

Here, m_1 , m_2 and m_c are the slope coefficients of V_i and V_c , as seen in Figure 2(a). K_{cfb} is the I/V conversion coefficient of the current detection circuit block depicted in Figure 1 and is constant once it is designed; D ($=V_{out}/V_{in}$) is the duty factor that shows the turn-on time of a transistor Mp out of one clock period of the control; and L is the inductance value of an external inductor in Figure 1. When V_{in} is constant, Equation (2) means that the compensation slope m_c should increase linearly as D increases. This results in the waveform for the compensation slope becoming quadratic, as shown in Figure 2(b), where the quadratic slope is added to the I/V converted voltage from the current that is proportional to the inductor current. When V_i reaches V_c , the output of the PWM comparator in Figure 1 becomes high, and this turns off the power transistor Mp.

III. THE USE OF THE QUADRATIC SLOPE

With the slope compensation, the small signal transfer function of the current feedback loop becomes similar to that of the second-order low-pass filter, as follows:

$$\frac{\Delta i_L}{\Delta v_c} = \frac{1}{K_{cfb}} \cdot \frac{1}{1 + \frac{2s}{\omega_n} \zeta + \frac{s^2}{\omega_n^2}} \quad (3)$$

where $\omega_n = \pi f_s$ is the natural frequency and it is at half the clock frequency. When the quadratic slope is used, the damping factor ζ is calculated as follows:

$$\zeta = \frac{\pi L}{2V_{in} K_{cfb}} \left(m_1 + 2m_c' DT_s \right) - \frac{\pi}{4} \quad (4)$$

where T_s is the clock period, m_1 is the slope shown by the dotted line in Figure 2(b) and is proportional to the inductor current, and m_c' is the coefficient of the quadratic slope. Here, m_1 is determined as follows:

$$m_1 = \frac{(V_{in} - V_{out}) K_{cfb}}{L} \quad (5)$$

We chose the damping factor ζ to be greater than 1/2 so that a second-order system such as a low-pass filter would not have the gain peak at all frequencies. In that case, m_c' is determined as follows:

$$m_c' \geq \frac{V_{in} K_{cfb} f_s}{2L} \left\{ 1 + \left(\frac{1}{\pi} - \frac{1}{2} \right) \frac{1}{D} \right\} \quad (6)$$

The right-hand side of equation (6) is at a maximum when D is 1, and therefore the following is chosen as the appropriate value:

$$m_c' = \frac{V_{in} K_{cfb} f_s}{2L} \quad (7)$$

Of course, equation (7) satisfies the criteria of equation (6). Then, the ζ value becomes $\pi/4$, i.e., constant. This means that the frequency characteristics of the current feedback loop become independent of V_{out} . However, it is obvious from equation (7) that m_c' needs to depend on V_{in} .

IV. VIN-DEPENDENT SLOPE GENERATION AND ITS CIRCUIT

The V_{in} dependency of m_c' in equation (7) is realized in the current detection and the slope compensation circuit, as shown in Figure 3. Mp and Mn in Figure 3 represent the output power transistors of a DC-DC converter. When Mp turns on to charge an external inductor L, SW1 turns on while SW2 turns off, and the voltage at terminal NLx is applied to the positive input terminal of operational amplifier 'op1'. The voltage at the negative input terminal of 'op1' becomes equal to the voltage at the positive input terminal due to the feedback operation performed by 'op1' and Mc2. Because the drain voltages of Mp and Mc1 are equal, and the gate of Mp is tied to the ground when Mp turns on, the inductor current that flows in Mp is mirrored to the current in Mc1 by the ratio of the transistor size. The current in Mc1 also flows in Rcd, and the replica voltage V_i , which is proportional to the inductor current, is obtained across Rcd.

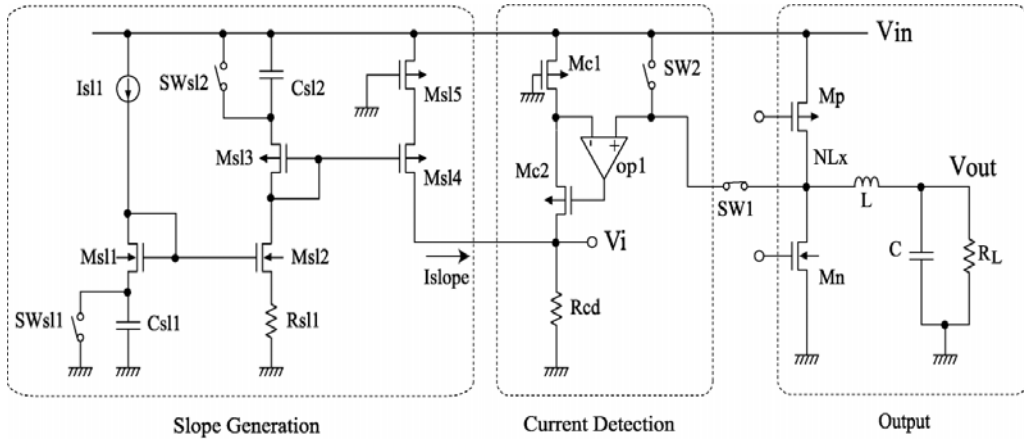


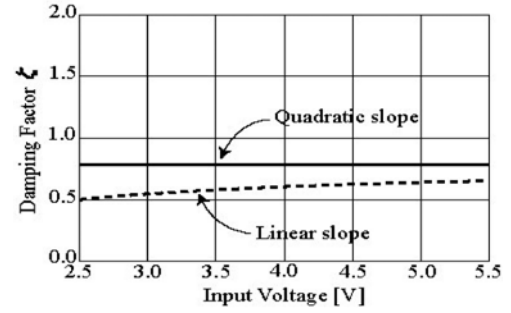
Fig. 3. A current detection and compensation slope generation circuit.

The quadratic compensation slope is generated by integrating a constant current twice using capacitors, as shown in Figure 3. The current I_{sl1} is constant, and the voltage across C_{sl1} increases with time when the switch SW_{sl1} turns off in synchronization with the turning on of the power transistor M_p . The voltage across C_{sl1} is copied to the voltage across R_{sl1} , and a current that increases linearly with time flows in R_{sl1} . The current in R_{sl1} flows in C_{sl2} , and the voltage across C_{sl2} becomes quadratic with time due to the time integration of the linearly increasing current in time by C_{sl2} . The turning off of the switch SW_{sl2} is also synchronized with the turning on of the power transistor M_p . Again, the voltage across C_{sl2} is copied to the voltage across M_{sl5} . As M_{sl5} is like a linear resistor, because it is driven in a triode region by its gate terminal being connected to the ground, the current I_{slope} becomes quadratic with time and is converted to the voltage by R_{cd} through M_{sl4} . The resultant quadratic slope voltage together with the voltage that is proportional to the inductor current becomes like that shown in Figure 2(b). The resistor value $R_{M_{sl5}}$ seen from the drain terminal of M_{sl5} in a triode region is approximated as follows:

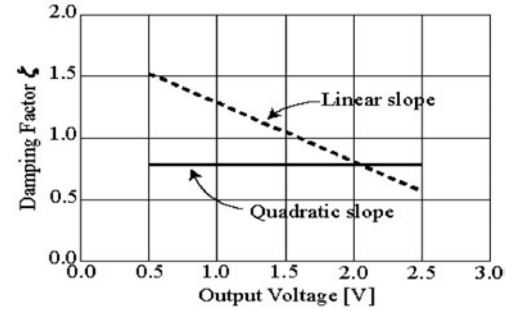
$$R_{M_{sl5}} \approx \frac{1}{\beta(V_{GS_{M_{sl5}}} - V_{th})} \approx \frac{1}{\beta V_{in}} \quad (8)$$

where β is the transconductance coefficient of M_{sl5} . Assuming V_{th} is small, $(V_{GS_{M_{sl5}}} - V_{th})$ is approximated to V_{in} because the gate of M_{sl5} is grounded. As the I_{slope} is determined by the division of the quadratic voltage change with time by the resistor in equation (8), we note that the coefficient of the I_{slope} and, therefore, the voltage across R_{cd} due to the I_{slope} becomes proportional to V_{in} . In this way, m_c' in equation (7) becomes linearly dependent on V_{in} .

Making the compensation slope quadratic and V_{in} -dependent enables the damping factor in equation (3) to remain constant for both V_{in} and V_{out} changes, as shown in Figure 4. When the linear slope is used, the damping factor ζ changes when the input and output voltages are chosen differently. As the damping factor governs the frequency characteristics of the current feedback loop, the frequency characteristics



(a) V_{in} dependency.



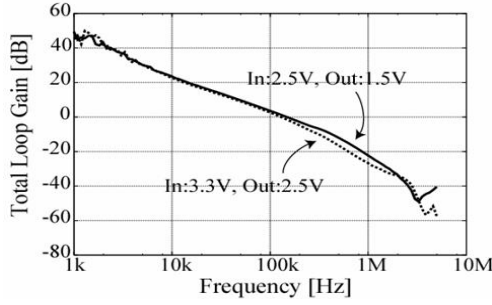
(b) V_{out} dependency.

Fig. 4. The effect of the quadratic and V_{in} -dependent slope.

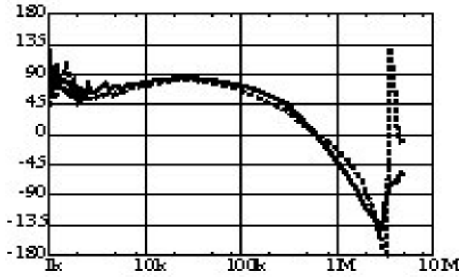
change depending on the input and output voltage settlement. In contrast to this, when the input-voltage-dependent quadratic slope is used, the damping factor becomes fixed at $\pi/4$. Completely unaltered frequency characteristics are expected.

V. EXPERIMENTAL RESULTS

To verify the effect of the quadratic and V_{in} -dependent compensation slope, we fabricated a test IC using a $0.35\text{-}\mu\text{m}$

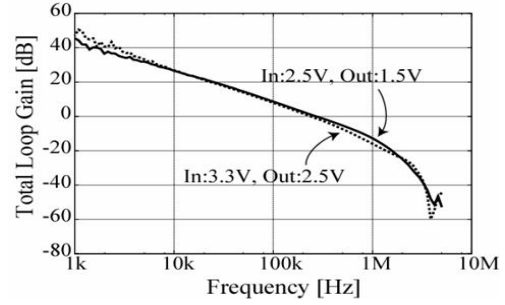


(a) Gain characteristics: The 0-dB bandwidths are at 150 kHz and 130 kHz.

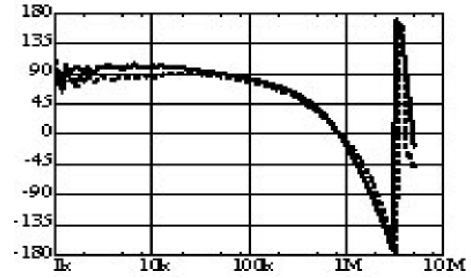


(b) Phase characteristics: The phase margins are 66° and 59° .

Fig. 5. Frequency characteristics of the total feedback loop with bandwidths of 150 kHz and 130 kHz.



(a) Gain characteristics: The 0-dB bandwidths are at 270 kHz and 240 kHz.



(b) Phase characteristics: The phase margins are 65° and 62° .

Fig. 6. Frequency characteristics of the total feedback loop with bandwidths of 270 kHz and 240 kHz.

CMOS process. Figure 5 and Figure 6 show the frequency characteristics of the total feedback loop in two different input and output voltage settings. The clock frequency was 5 MHz. Although the frequency characteristics of the current feedback loop were fixed, the frequency characteristics of the total feedback loop, which consisted of the combination of the frequency characteristics of the voltage feedback loop, the current feedback loop and the C and R_L together at the output in Figure 1, could be adjusted by using parameters C_e and R_e of the error amplifier in the voltage feedback loop and the external capacitor C at the output.

Figure 5 shows the gain and phase frequency characteristics when the frequency bandwidth is chosen to be approximately 140 kHz. Figure 6 shows the gain and phase frequency characteristics when the frequency bandwidth is chosen to be approximately 250 kHz. In each figure, (a) and (b), two curves are drawn. One is a curve with a 2.5-V input voltage and a 1.5-V output voltage, i.e., a duty ratio of 60%. The other curve has a 3.3-V input voltage and a 2.5-V output voltage with a duty ratio of 75%. With the two different input and output voltage settings described above, the frequency bandwidths were 150 kHz and 130 kHz and the phase margins were 66° and 59° , respectively, in the case shown in Figure 5. In Figure 6, the frequency bandwidths were increased to 270 kHz and 240 kHz with phase margins of 65° and 62° , respectively. In both cases

in Figures 5 and 6, no significant difference can be seen, even in curves of phase frequency characteristics for two different input and output voltage settings. It is obvious that constant frequency characteristics were obtained without depending on the input and output voltages.

VI. CONCLUSION

The use of the quadratic and input-voltage-dependent slope for a current feedback loop of the MOS current-mode buck DC-DC converter realized a wide loop bandwidth and completely unaltered frequency characteristics without depending on the input and output voltage changes.

REFERENCES

- [1] R.B.Ridley, "A New, Continuous-Time Model For Current-Mode Control," IEEE Trans. on Power Electronics, vol.6, no.2, pp.271-280, April 1991.
- [2] C.F.Lee and P.K.T.Mok, "A Monolithic Current-Mode CMOS DC-DC Converter With On-Chip Current-Sensing Technique," IEEE JSSC, vol.39, no.1, pp.3-14, January 2004.
- [3] K.Umimura, H.Sakurai, and Y.Sugimoto, "A CMOS Current-mode DC-DC Converter with Input and Output Voltage-Independent Stability and Frequency Characteristics Utilizing a Quadratic Slope Compensation Scheme," Proc. of ESSCIRC, pp.178-181, September 2007.
- [4] M.K.Kazimierczuk, "Transfer Function of Current Modulator in PWM Converters with Current-Mode Control," IEEE Trans. on Circuits and Systems-I:Fundamental Theory and Applications, vol.47, no.9, pp.1407-1412, September 2000.